Combining Synchronous Transit and Quasi-Newton Methods to Find Transition States

CHUNYANG PENG AND H. BERNHARD SCHLEGEL*
Department of Chemistry, Wayne State University, Detroit, MI 48202, USA

(Received 8 July 1993)

Dedicated to John A. Pople, recipient of the 1992 Wolf Prize in Chemistry

Abstract. A linear synchronous transit or quadratic synchronous transit approach is used to get closer to the quadratic region of the transition state and then quasi-newton or eigenvector following methods are used to complete the optimization. With an empirical estimate of the hessian, these methods converge efficiently for a variety of transition states from a range of starting structures.

INTRODUCTION

Equilibrium geometries and transition states are key elements in any endeavor to understand chemical reactivity and dynamics through the exploration of potential energy surfaces. Optimization algorithms for minima and first-order saddle points have been reviewed in a number of papers.[1-3] Gradient-based methods have made the search for equilibrium geometries for small and medium size molecules almost routine. However, transition states are often an order of magnitude more difficult to locate than minima, and the algorithms get into trouble more frequently than one would care to admit. To find a first-order saddle point (i.e., a transition structure), a maximum must be found in one (and only one) direction and minima in all other directions. Furthermore, the specific direction for maximization is usually not known in advance. Quasi-Newton methods are very robust and efficient for minimization, but when such methods are modified for locating saddle points, they have a much smaller radius of convergence.[1-3] For minima, qualitative theories of chemical structure are a valuable aid for choosing good starting geometries and suitable coordinate systems, whereas for transition states there is only the vague notion that the saddle point must lie somewhere between reactants and products. Various strategies have been devised to obtain a sufficiently good initial guess for the transition structure so that quasi-Newton methods will converge.[1-3] Based solely on local information, there is no unique way of moving uphill from either the reactants or products to reach a specific transition state since all directions away from a minimum go uphill. The shallowest ascent path or "walking along streambeds"[4] is a good choice for the uphill direction in many circumstances, but there is no guarantee that it will go to the desired transition state. The linear synchronous transit algorithm[5] (LST), which searches for a maximum along a linear path between reactants and products (in distant matrix space), is one method of getting near the transition state, but it frequently yields a structure with 2 or more negative eigenvalues. The quadratic synchronous transit method[5] (QST) is an improvement on the LST approach and searches for a maximum along a parabola connecting reactants and products, and for a minimum in all directions perpendicular to the parabola. Some versions of this method involve only energy calculations and converge slowly; others use gradients and are more efficient. [3,6]

H. Bernhard Schlegel received degrees from the University of Waterloo and Queen's University, Canada (Ph.D., 1975, with Saul Wolfe). After postdoctoral studies at Princeton University (with K. Mislow and L.C. Allen) and at Carnegie-Mellon University (with J.A. Pople) he joined the Merck, Sharp, and Dohme Research Labs. Since 1980 he has been a Professor of Chemistry at Wayne State University. His current research interests are geometry optimization, energy derivative methods, and application of quantum chemical calculations to organic chemistry.

Chunyang Peng received his degrees from Hunan University, China and from University of Texas, Austin (Ph.D., 1992, with J.E. Boggs). He is currently a postdoctoral fellow with H.B. Schlegel.

*Author to whom correspondence should be addressed.

Particularly noteworthy is the method implemented by Bell and Crighton.[3] After a maximum is found along a parabolic path between reactants and products, a minimum is found in the space *conjugate* to the path, rather than *orthogonal* to the path as is done in other implementations. In this paper we build on these ideas and our earlier efforts[7] to assemble a transition state searching method that combines a linear or quadratic synchronous transit approach for the first few steps in the optimization with a quasi-Newton-based eigenvector-following method[8] for rapid convergence toward the end of the optimization.

METHOD

Let $\vec{X}$, $\vec{R}$, and $\vec{P}$ be the coordinates of current point, the reactants, and the products, respectively. In the linear synchronous transit (LST) approach,[5] $\vec{X}$ is on a path that is a linear interpolation between $\vec{R}$ and $\vec{P}$. The quadratic synchronous transit (QST) method[5] uses a curved path through $\vec{X}$, $\vec{R}$, and $\vec{P}$. In both cases, a maximum is found along the path; QST adds a search for a minimum perpendicular or conjugate to the path. In the present approach, the tangent to the synchronous transit path (LST or QST) is used to guide the optimization to the quadratic region of the transition state. Then the tangent to the path is used to choose the best eigenvector for the ascent direction and an eigenvector-following or quasi-Newton method is used to complete the optimization.

Obtaining the Tangent Vector

The normalized tangent vector at $\vec{X}$ for the LST approach is simply:

$$\vec{T} = (\vec{P} - \vec{R}) / |\vec{P} - \vec{R}| \qquad (1)$$

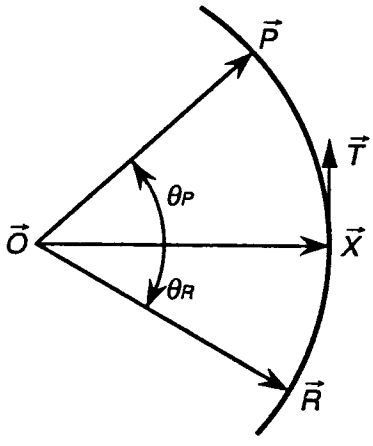

Fig. 1. An arc of a circle through the reactants, $\vec{R}$, the current point, $\vec{X}$, and the product, $\vec{P}$, is chosen as the path for the QST approach; $\vec{T}$ is the normalized tangent vector at $\vec{X}$.

For QST, the path is chosen to be an arc of a circle passing through $\vec{X}$, $\vec{R}$, and $\vec{P}$ rather than a parabola.[5] As illustrated in Fig. 1, if $\vec{O}$ is the origin of a circle of radius r passing through $\vec{X}$, $\vec{R}$, and $\vec{P}$, and $\vec{T}$ is the normalized tangent at $\vec{X}$ (i.e., $|\vec{X} - \vec{O}| = r$, $|\vec{T}| = 1$, $(\vec{X} - \vec{O}) \cdot \vec{T} = 0$), then

$$\vec{R} = \vec{O} + (\vec{X} - \vec{O}) \cos\theta_R + r\vec{T} \sin\theta_R \qquad (2)$$

$$\vec{R} - \vec{X} = (\vec{X} - \vec{O})(\cos\theta_R - 1) + r\vec{T} \sin\theta_R \qquad (3)$$

$$|\vec{R} - \vec{X}|^2 = 2r^2(1 - \cos\theta_R) \qquad (4)$$

$$(\vec{R} - \vec{X}) / |\vec{R} - \vec{X}|^2 = -(\vec{X} - \vec{O})/2r + \vec{T} \sin\theta_R / 2r(1 - \cos\theta_R) \qquad (5)$$

Likewise,

$$(\vec{P} - \vec{X}) / |\vec{P} - \vec{X}|^2 = -(\vec{X} - \vec{O})/2r + \vec{T} \sin\theta_P / 2r(1 - \cos\theta_P) \qquad (6)$$

(note that $\theta_R < 0$, $\theta_P > 0$). The un-normalized tangent can then be calculated as

$$(\vec{P} - \vec{X}) / |\vec{P} - \vec{X}|^2 - (\vec{R} - \vec{X}) / |\vec{R} - \vec{X}|^2$$
$$= \vec{T}(\sin\theta_P / 2r(1 - \cos\theta_P) - \sin\theta_R / 2r(1 - \cos\theta_R)) \qquad (7)$$

and the normalized tangent is

$$\vec{T} = a((\vec{P} - \vec{X}) / |\vec{P} - \vec{X}|^2 - (\vec{R} - \vec{X}) / |\vec{R} - \vec{X}|^2)$$
$$a^2 = |\vec{R} - \vec{X}|^2 |\vec{P} - \vec{X}|^2 /$$
$$(|\vec{R} - \vec{X}|^2 + |\vec{P} - \vec{X}|^2 - 2(\vec{R} - \vec{X}) \cdot (\vec{P} - \vec{X})) \qquad (8)$$

Transforming the Tangent Vector

The tangent can be computed using eq 8 for cartesian coordinates, internal coordinates (nonredundant or redundant[9]), or distance matrix coordinates (i.e., all $n(n-1)/2$ interatomic distances for an n atom molecule). If distance matrix coordinates are used (as is typical in LST or QST calculations[5]), the tangent must be transformed to the coordinates used for the optimization (usually cartesian or internal coordinates). The transformation from distance matrix to cartesian coordinates is:

$$\vec{T}_x = (\mathbf{M}\mathbf{B}_d^t\mathbf{B}_d\mathbf{M})^{-1}\mathbf{M}\mathbf{B}_d^t\vec{T}_d \qquad (9)$$

where $\mathbf{B}_d$ is the Wilson B matrix[10] relating cartesian displacements to distance matrix coordinates and $\mathbf{M}$ is any matrix. In the Z-matrix orientation,[11] coordinates x_1, y_1, z_1, x_2, y_2, y_3 are constrained to be zero and a suitable choice for $\mathbf{M}$ is the identity matrix with zeros on the diagonal corresponding to the constrained coordinates. The transformation from cartesians to internal coordinates is straightforward:

$$\vec{T}_q = \mathbf{B}_q\vec{T}_x \qquad (10)$$

where $\mathbf{B}_q$ is the Wilson B matrix relating cartesian displacements to the internal coordinates used in the optimization.

Controlling the Step Size and Search Direction

If the starting geometry is far from the quadratic region, it is necessary to climb in the direction of the tangent vector for several steps to get near the maximun along the LST or QST path before any minimization steps are taken. The gradient and the updated Hessian are used to determine the step size in the tangent direction according to the eigenvector-following procedure,[8]

$$\Delta\vec{x} = -\vec{v}_k(\vec{v}_k{}^t\vec{g})/(b_k-\lambda_0);$$

$$\lambda_0 = (b_k+\sqrt{b_k{}^2+4(\vec{v}_k{}^t\vec{g})^2})/2 \qquad (11)$$

where $\Delta\vec{X}$ is the displacement, $\vec{g}$ is the gradient, $\vec{v}_k$ is the eigenvector of the Hessian that is chosen as the ascent direction, and b_k is the associated eigenvalue. When the current point is suitably close to the maximum in the LST or QST path, the optimization is switched to the eigenvector-following method[8] in the full space of the variables (i.e., the regular transition state optimization method in the GAUSSIAN series of programs[11]). One of the eigenvectors of the updated Hessian is used as the ascent direction. Normally the one with the lowest eigenvalue is chosen. However, if another eigenvector has a large overlap with the tangent to the LST or QST path, then this eigenvector is chosen as the ascent direction.

Combined Synchronous Transit / Eigenvector-following Algorithm

The following procedure is used for each step in a transition structure optimization:

1. Update the Hessian.
2. Compute the tangent vector using eq 1 for an LST path or eq 8 for a QST path. If distance matrix coordinates are being used to define the LST or QST path, transform the tangent vector to the optimization coordinates via eqs 9 and 10.
3. Determine whether this is a climbing step or an eigenvector-following step:
   (a) Always choose climbing for steps 1 and 2.
   (b) For step 3 or 4 choose climbing if the estimated displacement along the tangent vector is greater than the threshold (default 0.05 au); otherwise, choose eigenvector following.
   (c) Always choose eigenvector following for step 5 and beyond.
4. (a) For a climbing step, compute the displacement along the tangent according to eq 11. No displacement is made along any direction perpendicular to the path.
   (b) For an eigenvector-following step, compute the overlap between the tangent and the eigenvectors of the Hessian; if the overlap is greater than the cutoff (default 0.8), then switch the eigenvectors so as to follow the one with the maximum overlap with the tangent; otherwise, follow the eigenvector with the smallest eigenvalue.
5. If the displacement is larger than the maximum step size, scale the step back to the maximum (default 0.3 au).
6. Test for convergence using the standard criteria in

Table 1. Comparison of the number of steps taken for various transition state optimizations[1]

Reaction and starting geometry[2]	Regular[3]		LST[4] internal	LST[4] dist. mat	QST[5] internal	QST[5] dist. mat
	(a)	(b)	(c)	(d)	(e)	(f)
(1) $CH_4+F\rightarrow CH_3+HF$ (4 degrees of freedom)						
(i)	6	8	6	7	6	8
(ii)	10	10	9	9	10	9
(iii)	12	fail	13	20	11	16
(2) $CH_3O\rightarrow CH_2OH$ (6 degrees of freedom)						
(i)	12	fail	9	9	9	9
(ii)	15	11	12	13	12	13
(iii)	11	10	12	10	12	12
(3) $SiH_2+H_2\rightarrow SiH_4$ (6 degrees of freedom)						
(i)	11	fail	11	11	11	11
(ii)	10	11	12	11	12	12
(iii)	11	fail	12	12	10	12
(4) $CH_3CH_2F\rightarrow CH_2{=}CH_2+HF$ (11 degrees of freedom)						
(i)	16	23	24	15	15	15
(ii)	23	18	16	21	18	18
(iii)	13	14	13	13	15	14
(5) Diels–Alder reaction (21 degrees of freedom)						
(i)	56	18	22	18	23	18
(ii)	65	22	43	17	fail	20
(iii)	fail	30	14	15	14	14
(6) Claisen rearrangement (36 degrees of freedom)						
(i)	38	20	13	12	15	15
(ii)	25	fail	16	19	17	17
(7) Ene reaction (39 degrees of freedom)						
(i)	fail	31	26	28	28	27
(ii)	54	32	36	31	26	22

[1]Total number of energy+gradient steps, including any preliminary steps used to estimate parts of the hessian.
[2]See Fig. 1 for definition of internal coordinates; (i) is the starting geometry given in Fig. 1. For reactions 1–5, (ii)$\vec{X}'\approx(\vec{X}+\vec{R})/2$ and (iii)$\vec{X}''\approx(\vec{X}+\vec{P})/2$; for reactions (6) and 7, (ii) uses a product-like set of internal coordinates.
[3]Using the regular transition state optimization in GAUSSIAN 92 (a) with 2–4 preliminary steps to estimate key parts of the Hessian and (b) without any preliminary steps.
[4]LST based on eqs 1, 9, and 10 using (c) internal coordinates and (d) distance matrix coordinates, *with no preliminary steps.*
[5]QST based on eqs 8–10 using (e) internal coordinates and (f) distance matrix coordinates, *with no preliminary steps.*

GAUSSIAN[11] — maximum component of the gradient must be less than 0.00045 au, root mean square of the gradient must be less than 0.00030 au, maximum component of the displacement must be less than 0.0018 au, and root mean square of the displacement must be less than 0.0012 au. If all 4 conditions are satisfied, stop; otherwise, continue the optimization.

RESULTS AND DISCUSSION

Table 1 contains a summary of several transition structure searches for a number of representative reactions. All calculations were carried out with a modified version of the GAUSSIAN system of programs.[11] The HF/3-21G level of theory was used to demonstrate the performance of the optimization methods; the results with other levels of theory should be similar.

A number of reactions have been considered in order to sample a range of transition states that might be encountered in typical applications. Reactions 1–4 are relatively simple but have saddle-point geometries characteristic of large classes of transition states. Reactions 5–7 have more challenging transition states that combine the problems of extensive bonding rearrangement with the difficulties of optimizing cyclic structures:

(1) an atom abstraction, $CH_4+F\rightarrow CH_3+HF$ (this is also representative of S_N2 reactions and other group transfer reactions);
(2) a 1,2 hydrogen shift, $CH_3O\rightarrow CH_2OH$ (a simple model for more general 1,*n* group shifts);
(3) a 1,1 elimination or insertion, $SiH_4\rightarrow SiH_2+H_2$ (an example for reactions involving 3-membered rings in the transition state);
(4) a 1,2 addition or cis elimination, $CH_2=CH_2+HF\rightarrow CH_3CH_2F$ (a 4-membered ring transition state);
(5) $CH_2=CH_2+CH_2=CH-CH=CH_2\rightarrow$ cyclohexene (a Diels–Alder reaction);
(6) $CH_2=CH-CH_2-O-CH=CH_2\rightarrow CH_2=CH-CH_2-CH_2-CH=O$ (a Claisen rearrangement);
(7) $CH_2=CH_2+CH_2=CH-CH_3\rightarrow CH_2=CH-CH_2-CH_2-CH_3$ (an ene reaction).

The starting geometries and optimized transition states are shown in Fig. 2. The input consists of the regular Z matrix definition of the internal coordinates of the molecule. The variables section of the input has been modified so that the reactant and product geometries can be specified, as well as the initial estimate of the transition structure. For each variable, the 3 values correspond to $\bar{X}$, $\bar{R}$, and $\bar{P}$, respectively. If cartesian or redundant internal coordinates are used for the optimization, then there is no need to use the same Z-matrix for $\bar{X}$, $\bar{R}$, and $\bar{P}$, and they could be entered as 3 separate structures. The parameters for $\bar{R}$ and $\bar{P}$ are estimates of the reactant and product geometries (for bimolecular reactions, the separation between fragments has been chosen in the range 2–3 Å, depending on the nature of the bonds formed or broken). For reactions 1–5 three sets of starting values for $\bar{X}$ were used in each case. The first is shown in Fig. 2 and is a reasonable estimate of the transition structure, typically about halfway between $\bar{R}$ and $\bar{P}$; in the second, $\bar{X}$ is significantly closer to the reactants and in the third, $\bar{X}$ is closer to the products (about 1/4 and 3/4 of the way between reactants and products, respectively). For reactions 6 and 7, two different sets of internal coordinates were used for the transition state search, one reactant-like and the other product-like. In both cases, the starting geometry $\bar{X}$ was chosen to be about halfway between $\bar{R}$ and $\bar{P}$. Proper use of dummy atoms can often accelerate the convergence of transition state optimizations. However, to challenge the present optimization methods, no special efforts were made to use dummy atoms unless demanded by symmetry or by linear bond angles. The Z-matrices shown in Fig. 2 are not recommended for general use in optimizing these transition states; ref 12 offers suggestions of ways to construct better coordinate systems for transition states.

Each of the transition structure searches was carried out in six different ways:

(a) The regular algorithm in Gaussian (Hessian update and linear search according to ref 7, eigenvector following as in refs 4 and 8, empirical estimate of the Hessian as outlined in ref 13) with 2–4 preliminary steps to estimate key elements of the Hessian;
(b) The regular algorithm in Gaussian but with no preliminary gradient steps;
(c) LST path in the internal (Z-matrix) variable space (eq 1);
(d) LST path in distance matrix space (eqs 1, 9,10);
(e) QST path in the internal (Z-matrix) variable space (eq 8);
(f) QST path in distance matrix space (eqs 8–10).

In all LST and QST cases, only an empirical valence force field was used for the initial estimate of the Hessian[13] and no preliminary gradient calculations were used to improve the initial estimate of the Hessian.

The regular transition structure optimization in Gaussian performs well provided that several preliminary gradient calculations are used to numerically compute key rows and columns of the Hessian. This is sufficient to determine the direction of the transition vector so that eigenvector following reaches the transition state. The steps listed in Table 1 include these preliminary steps. However, when no preliminary steps are taken, a quarter of the regular optimizations fail, particularly if the starting geometry is too close to the reactants or products. This implies that a good estimate of the transition vector is needed for the regular optimization to behave properly.

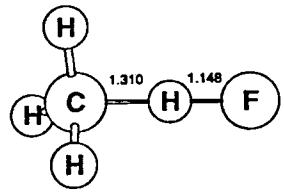


```
C
H 1 CH0
H 1 CH 2 A1
H 1 CH 2 A1 3 120.
H 1 CH 2 A1 3 -120.
X 2 1.0 1 90.0 3 180.0
F 2 HF 6 90.0 1 180.0

CH0  1.25   2.00  1.08
HF   1.25   0.92  2.00
A1   100.   90.0  109.48
CH   1.08   1.08  1.08
```

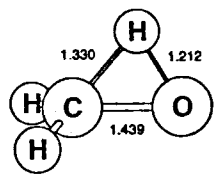


```
C
O 1 R1
H 1 R2 2 A2
H 1 R3 2 A3 3 D3
H 1 R3 2 A3 3 -D3

R1 1.48 1.48 1.48
R2 1.40 1.06 1.90
R3 1.08 1.08 1.08
A2  70.  110.  30.
A3 110. 110. 110.
D3 120. 120. 120.
```

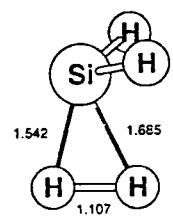


```
Si
X  1  1.0
H  1  HSi  2  ASi
H  1  HSi  2  ASi  3  180.0
H  1  HSi5 2  HSiX 3  90.0
H  1  HSi6 5  HSiH 2  180.0

HSi   1.48 1.48 1.48
ASi   55.0 55.0 55.0
HSi5  1.80 2.00 1.48
HSi6  1.80 2.00 1.48
HSiX  95.0 80.0 125.2
HSiH  50.0 22.0 109.5
```

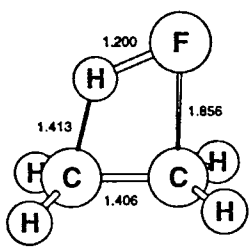


```
C
C 1 CC
H 1 HC  2 AH
F 2 FC  1 AF 3 0.
H 1 HC1 2 A1  4 D1
H 1 HC1 2 A1  4 -D1
H 2 HC2 1 A2  4 D2
H 2 HC2 1 A2  4 -D2

CC   1.43  1.54  1.32
HC   1.50  1.08  2.50
FC   1.90  1.41  2.50
HC1  1.08  1.08  1.08
HC2  1.08  1.08  1.08
AH   100.  110.  85.
AF   100.  110.  85.
A1   115.  110.  120.
A2   115.  110.  120.
D1   105.  120.  90.
D2   105.  120.  90.
```

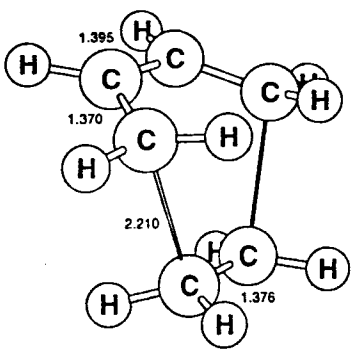


```
C
C 1 RCC1
C 1 RCC2 2 ACC2
C 2 RCC2 1 ACC2 3  0.0
C 3 RCC3 1 ACC3 2  DCC3
C 4 RCC3 2 ACC3 1  -DCC3
H 1 RCH1 2 ACH1 3  DCH1
H 2 RCH1 1 ACH1 4  -DCH1
H 3 RCH2 1 ACH2 2  DCH2
H 3 RCH3 1 ACH3 2  DCH3
H 4 RCH2 2 ACH2 1  -DCH2
H 4 RCH3 2 ACH3 1  -DCH3
H 5 RCH4 6 ACH4 3  DCH4
H 5 RCH5 6 ACH5 3  DCH5
H 6 RCH4 5 ACH4 4  -DCH4
H 6 RCH5 5 ACH5 4  -DCH5

RCC1  1.41  1.50  1.32
RCC2  1.41  1.32  1.54
RCC3  2.00  3.00  1.54
ACC2  120.  120.  120.
ACC3  100.  90.  100.
DCC3  58.  73.  53.
RCH1  1.08  1.08  1.08
RCH2  1.08  1.08  1.08
RCH3  1.08  1.08  1.08
RCH4  1.08  1.08  1.08
RCH5  1.08  1.08  1.08
ACH1  120.  120.  120.
ACH2  115.  120.  110.
ACH3  115.  120.  110.
ACH4  115.  120.  110.
ACH5  115.  120.  110.
DCH1  180.  180.  180.
DCH2  180.  180.  180.
DCH3  -30.  0.  -60.
DCH4  105.  90.  120.
DCH5  -105.  -90.  -120.
```

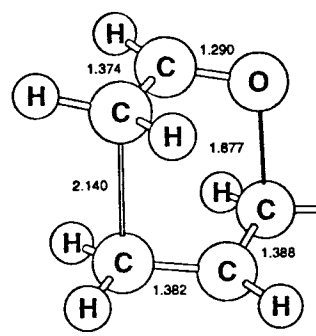


```
C
C 1 R1
C 2 R2 1 A2
O 3 R3 2 A3 1 D3
C 4 R4 3 A4 2 D4
C 5 R5 4 A5 3 D5
H 1 RH1 2 AH1 3 DH1
H 1 RH2 2 AH2 3 DH2
H 2 RH3 1 AH3 3 DH3
H 3 RH4 2 AH4 1 DH4
H 3 RH5 2 AH5 1 DH5
H 6 RH6 5 AH6 4 DH6
H 6 RH7 5 AH7 4 DH7
H 5 RH8 6 AH8 4 DH8

R1 1.420 1.32 1.52
R2 1.405 1.51 1.32
R3 2.008 1.44 2.457
R4 1.310 1.41 1.21
R5 1.410 1.32 1.52
A2 120.  120.  120.
A3 101.1 109.5 93.67
A4 103.5 109.5 97.42
A5 120.  120.  120.
D3 -66.8 -75.  -58.7
D4 56.6  60.  52.9
D5 -67.8 -75.  -60.65

RH1 1.09 1.09 1.09
RH2 1.09 1.09 1.09
RH3 1.09 1.09 1.09
RH4 1.09 1.09 1.09
RH5 1.09 1.09 1.09
RH6 1.09 1.09 1.09
RH7 1.09 1.09 1.09
RH8 1.09 1.09 1.09
AH1 115. 120. 109.5
AH2 115. 120. 109.5
AH3 120. 120. 120.
AH4 115. 109.5 120.
AH5 115. 109.5 120.
AH6 115. 109.5 120.
AH7 115. 109.5 120.
AH8 120. 120. 120.
DH1 -30.  0.  -60.
DH2 180. 180. 180.
DH3 180. 180. 180.
DH4 180. 180. 180.
DH5 30.  60.  0.
DH6 180. 180. 180.
DH7 -30.  0.  -60.
DH8 180. 180. 180.
```

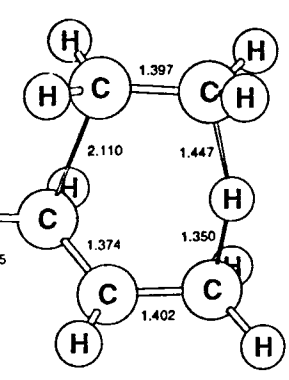


```
C
C 1 R1
C 2 R2 1 A2
C 3 R3 2 A3 1 D3
C 4 R4 3 A4 2 D4
H 1 RH1 2 AH1 3 DH1
H 1 RH12 2 AH12 6 DH2
H 1 RH3 2 AH3 6 DH3
H 2 RH4 3 AH4 1 DH4
H 3 RH5 2 AH5 1 DH5
H 3 RH6 2 AH6 1 DH6
H 4 RH7 5 AH7 3 DH7
H 4 RH8 5 AH8 12 DH8
H 5 RH9 4 AH9 12 DH9
H 5 RHA 4 AHA 12 DHA

R1 1.41 1.51 1.32
R2 1.41 1.32 1.51
R3 1.77 2.00 1.54
R4 1.43 1.32 1.54
A2 120. 120. 120.
A3 109.5 109.5 109.5
A4 109.6 109.6 109.6
D3 60. 90. 90.
D4 -30. -30. -30.
RH1 1.515 1.08 1.951
RH2 1.08 1.08 1.08
RH3 1.08 1.08 1.08
RH4 1.08 1.08 1.08
RH5 1.08 1.08 1.08

RH6 1.08 1.08 1.08
RH7 1.08 1.08 1.08
RH8 1.08 1.08 1.08
RH9 1.08 1.08 1.08
RHA 1.08 1.08 1.08
AH1 92.1 109.5 75.61
AH2 115. 109.5 120.
AH3 115. 109.5 120.
AH4 120. 120. 120.
AH5 115. 120. 109.5
AH6 115. 120. 109.5
AH7 115. 120. 109.5
AH8 115. 120. 109.5
AH9 115. 120. 109.5
AHA 115. 120. 109.5

DH1 -59.37 -50. -68.75
DH2 95. 120. 70.
DH3 -115. -120. -110.
DH4 180. 180. 180.
DH5 -15. 0. -30.
DH6 195. 180. 210.
DH7 105. 90. 120.
DH8 150. 180. 120.
DH9 0. 0. 0.
DHA 210. 180. 240.
```

Fig. 2. Initial geometries, internal coordinates, and optimized transition structures for $CH_3+HF\rightarrow CH_4+F$, $H_3CO\rightarrow H_2COH$, $SiH_2+H_2\rightarrow SiH_4$, $CH_3CH_2F\rightarrow CH_2CH_2+HF$, a Diels–Alder reaction, a Claisen rearrangement, and an ene reaction. The 3 values listed for each variable correspond to the initial estimate of the transition state, $\bar{X}$, the approximate reactants, $\bar{R}$, and the approximate products, $\bar{P}$, respectively.

The LST and QST transition structure searches without preliminary steps to estimate the Hessian require about the same number of steps as the regular optimization with preliminary steps. In a few cases, distance matrix coordinates behave somewhat better (ethylene + butadiene (ii)); more frequently, there is very little difference between LST and QST and between internal coordinates and distance matrix coordinates. Apparently, only the general direction of the path through the transition state is needed. The curvature of the path and the coordiante space for the approximate path are of lesser importance. Because the radius of the path is typically fairly large ($r > 3$ au), the short linear steps along the path (limited to a maximum of 0.3 au in the present case) do not deviate significantly from the QST path, and there is no need to take curved steps (note that the tangent to the LST or QST path is redetermined at each step using the current point in combination with $\vec{R}$ and $\vec{P}$). After some experimentation, we found it best to require a minimum of 2 and maximum of 4 climbing steps before changing to quasi-Newton optimization or eigenvector following. In subsequent steps, it was best not to switch the ascent direction from the eigenvector with the smallest eigenvalue unless there was another eigenvector with greater than 0.8 overlap with the tangent vector.

In summary, the scheme outlined above starts with approximations for the reactants, products, and transition structure, and an empirical estimate of the Hessian, and proceeds efficiently and reliably to an optimized transition state by combining the synchronous transit approach and eigenvector-following method.

Acknowledgments. We wish to thank Wayne State University and the Pittsburgh Supercomputer Center for computer time. This work was supported by a grant from the National Science Foundation (CHE 90-20398).

REFERENCES

(1) Schlegel, H.B. *Adv. Chem. Phys.* 1987, **67**: 249.
(2) Head, J.D.; Zerner, M.C. *Adv. Quantum Chem.* 1989, **20**: 239.
(3) Bell, S.; Crighton, J.S. *J. Chem. Phys.* 1984, **80**: 2464.
(4) Simons, J.; Nichols, J. *Int. J. Quantum Chem., Quantum Chem. Symp.* 1990, **24**: 263, and references therein.
(5) Halgren, T.A.;Lipscomb, W.N. *Chem. Phys. Lett.* 1977, **49**: 225.
(6) Jensen, A. *Theor. Chim. Acta* 1983, **63**: 269.
(7) Schlegel, H.B. *J. Comput. Chem.* 1982, **3**: 214.
(8) Baker, J.; Hehre, W.J. *J. Comput. Chem.* 1991, **12**: 606.
(9) Pulay, P.; Fogarasi, G. *J. Chem. Phys.* 1992, **96**: 2856. Fogarasi, G.; Zhou, X.; Taylor, P.; Pulay, P. *J. Am. Chem. Soc.* 1992, **114**: 8191.
(10) Wilson, E.B.; Decius, J.C.; Cross, P.C. *Molecular Vibrations*; McGraw-Hill: New York, 1955.
(11) GAUSSIAN 92. Frisch, J.M.; Trucks, G.W.; Head-Gordon, M.; Gill, P.M.W.; Foresman, J.B.; Johnson, B.G.; Schlegel, H.B.; Robb, M.A.; Replogle, E.S.; Gomperts, R.; Andrés, J.L.; Raghavachari, K.; Binkley, J.S.; Gonzalez, C.; Martin, R.L.; Fox, D.J.; DeFrees, D.J.; Baker, J.; Stewart, J.J.P.; Pople, J.A. Gaussian, Inc., Pittsburgh, PA, 1992.
(12) Schlegel, H.B. In *New Theoretical Concepts for Understanding Organic Reactions;* Bertrán, J., Ed.; Kluwer: Dordrecht, 1989, NATO-ASI series C 267, pp. 33–53.
(13) Schlegel, H.B. *Theor. Chim. Acta* 1984, **66**: 333.